Signatures of kinetic instabilities in the solar wind

Lorenzo Matteini[1,2], Petr Hellinger[3], Bruce E. Goldstein[4], Simone Landi[2], Marco Velli[2,4], and Marcia Neugebauer[5]

Abstract. An analysis of ion non-thermal properties in the fast solar wind based on Ulysses data is reported. The radial evolution of the main proton moments (density, temperature, and drift velocities) and their empirical correlations with other plasma parameters are investigated in detail and compared with theoretical expectations. The stability of the plasma is studied against different ion kinetic instabilities driven by ion temperature anisotropies and differential velocities, focusing on the identification of possible signatures of relevant instabilities in the observed core-beam structure of proton distributions. The temperature anisotropy of the total proton distribution appears to be constrained by fire hose instabilities, in agreement with previous studies, while if considered separately, beam and core populations exhibit opposite anisotropies, with core protons characterized by perpendicular temperatures larger than the parallel ones, possibly (marginally) unstable for ion-cyclotron instability. The evolution with distance of the drift velocity between the secondary population and the main core is found to be non adiabatic, leading to the identification of a marginal stability path of a magnetosonic ion-beam instability. As a conclusion, we find that a large fraction of the proton distributions observed by Ulysses display signatures of either a beam or a fire hose instability, suggesting that such kinetic processes play an important role in regulating the solar wind thermal energetics during the plasma expansion.

1. Introduction

The weakly collisional solar wind plasma is far from thermodynamical equilibrium. Several non-thermal features are observed in the ion velocity distribution functions, in particular temperature anisotropies and ion differential streaming [*Marsch et al.*, 1982a, b]. Such effects are more pronounced in the fast solar wind, where protons often consist of two populations, a more dense dominant core and faster less dense beam, characterized by temperature anisotropies and differential velocities varying with the radial distance. Closer to the Sun, a temperature anisotropy $T_\perp > T_\parallel$ (parallel and perpendicular temperatures, $T_\parallel$ and $T_\perp$, are defined with respect to the direction of the ambient magnetic field) is systematically observed in proton cores, while such an anisotropy relaxes with radial distance and $T_\perp \lesssim T_\parallel$ at 1 AU [e.g., *Matteini et al.*, 2007]. At the same time, the drift velocity between the core and beam proton populations between 0.3 and 1 AU is observed to decrease with radial distance [*Marsch et al.*, 1982b]. Similarly, also the relative proton-alpha drift speed decreases with distance [*Marsch et al.*, 1982a; *Neugebauer et al.*, 1996].

The presence of temperature anisotropy is a source of free energy for many different plasma instabilities; when this exceeds a certain threshold the systems reacts generating unstable fluctuations that scatter particles towards a more isotropic configuration. In this process, the dominant temperature direction loses some energy that is transferred to the other component and to electromagnetic fluctuations, so that the global kinetic energy decreases; the local power of fluctuations increases while particles are cooled down. In the last years several studies have addressed the issue of comparing the level of observed particle temperature anisotropies in the solar wind with theoretical instability thresholds, at various heliocentric distances and for different spacecraft. Investigations on protons [*Kasper et al.*, 2002; *Hellinger et al.*, 2006; *Marsch et al.*, 2006; *Matteini et al.*, 2007; *Bale et al.*, 2009] have revealed the presence of apparent observational boundaries in the distribution of the measured temperature anisotropies. Similar boundaries are also observed for alpha particles [*Maruca et al.*, 2012] and possibly electrons [*Štverák et al.*, 2008], even if for the latter Coulomb collisions play an important role and are largely responsible for the thermal evolution of the particles [*Landi et al.*, 2012]. These observational limits are relatively in good agreement with the theoretical constrains derived from linear theory of plasma instabilities. This suggests that those kinetic processes, as fire hose, ion-cyclotron and mirror instabilities, play a role in the regulation of the solar wind thermodynamics along the expansion. Kinetic numerical simulation studies that include the effect of the radial expansion of the solar wind on the plasma [*Hellinger et al.*, 2005; *Matteini et al.*, 2006; *Hellinger and Trávníček*, 2008; *Matteini et al.*, 2012] confirm this interpretation. Moreover, the analysis of magnetic fluctuations in the solar wind reveals an enhancement of magnetic power when the plasma is observed to be close to the instability thresholds [*Bale et al.*, 2009; *Wicks et al.*, 2013], suggesting a presence of a wave activity excited by temperature-anisotropy driven instabilities close to the ion inertial length scale and blended together with the solar wind turbulence.

The possibility of exciting temperature-anisotropy driven instabilities depends on many plasma parameters, but primarily on the plasma beta (besides the temperature anisotropy); consequently it is has become common to plot the instability analysis in a ($\beta_\parallel$,$T_\perp/T_\parallel$) plane [cf., *Gary et al.*, 2001]. The dominant instabilities are electromagnetic and typically need large betas (especially fire hoses

[1]Imperial College London, UK
[2]Dipartimento di Astronomia e Scienza dello Spazio, Università degli Studi di Firenze, Italy
[3]Astronomical Institute, AS CR, Prague, Czech Republic.
[4]Jet Propulsion Laboratory, California Institute of Technology, Pasadena, California, US
[5]Lunar and Planetary Laboratory, University of Arizona, Tucson, US

0148-0227/13/$9.00

which need substantial $\beta \gtrsim 1$) their roles in the solar wind plasma are expected to change with distance as both the plasma beta and the temperature anisotropy depend on radial distance. As a consequence, plasma that is stable at a given heliocentric distance will not remain stable and confined within the same region of the parameter space at larger distances. In the slow solar wind, due to its very variable conditions (and possibly due to a non negligible collisionality), signatures of an evolution path in the parameter space are difficult to find; on the contrary, a clear path can be recovered in fast wind observations, as demonstrated by *Matteini et al.* [2007].

Besides the observed apparent bounds on ion properties, some correlations between different ion quantitities are often observed. *Marsch et al.* [2004] reported the presence of an anti-correlation between the anisotropy and the parallel beta of the proton cores in the fast wind between 0.3 and 1 AU. This anti-correlation departs from the double-adiabatic prediction, hence suggesting the presence of a perpendicular heating contrasting the rapid cooling of protons in the direction transverse to the mean magnetic field imposed by particle magnetic moment conservation ($\mu = v_\perp^2/B$, so $v_\perp^2 \propto B \propto R^{-2}$ in a radial magnetic field). *Tu et al.* [2004] reported for the first time the existence of a correlation between the relative core-beam drift velocity in proton distributions and the core parallel beta in Helios data, while *Goldstein et al.* [2010] have found that there is a good correlation between the anisotropy of the beam population and the core-beam relative drift, normalized to the local Alfvén speed. Such findings seem to suggest that a tight connection exists among these parameters and support the idea that different plasma processes are at work in shaping globally the proton distributions. These different correlations are not well understood; some of the correlations may be related to kinetic instabilities and boundaries imposed by these instabilities in the multidimensional plasma parameter space.

Concerning theoretical modeling, mechanisms for the generation of ion beams related to parametric instabilities of Alfvén waves at parallel [*Araneda et al.*, 2008, 2009; *Matteini et al.*, 2010b] and oblique propagation [*Matteini et al.*, 2010a] have been recently proposed. In this framework, the acceleration of beams appear to be more efficient at low plasma beta, thus in regions closer to the Sun. This is consistent with the idea that the generation of ion differential velocities (and large temperature anisotropies) occurs within few solar radii [e.g. *Antonucci*, 2006], and that at larger distance we observe their relaxation during the solar wind expansion. Such a relaxation appears however complicated, as discussed above.

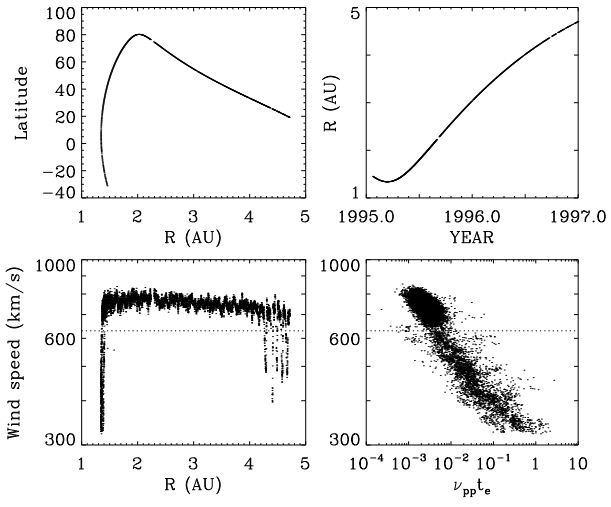

Figure 1. Overview of the Ulysses data used in this work. Top panels: Heliographic latitude as a function of the radial distance R (left), heliocentric distance as a function of time (right). Bottom panels: solar wind bulk velocity as a function of R (left) and estimated collisionality (right).

Proton beams measured by Helios between 0.3 and 1 AU show densities of the order of n_b/n_e ∼10-20%, with few cases with n_b/n_e >30% [*Marsch et al.*, 1982b], while Ulysses observations report secondary proton beams that are remarkably larger [*Goldstein et al.*, 2000; *Goldstein et al.*, 2010], with mean densities of around 30% and sometimes the relative density of the secondary population becomes comparable to the one of the core. This suggests the presence of an evolution with distance of the proton core-beam structure, possibly mediated by wave-particle interactions and ion-beam instabilities[*Marsch and Livi*, 1987; *Daughton and Gary*, 1998; *Daughton et al.*, 1999]. However, there were differences in the analysis techniques that would account for differences. *Marsch et al.* [1982b] required that the beams be clearly distinguishable, whereas *Goldstein et al.* [2000]; *Goldstein et al.* [2010] included cases in which a two beam fit was superior to a single beam, such as a shoulder on a distribution.

According to the picture described, several instabilities may be at work in the solar wind, driven by proton total, core, and beam temperature anisotropy, proton core-beam drift, alpha anisotropy, and alpha-proton drift. In this paper, we focus on proton properties measured by the Ulysses spacecraft and we discuss a first large analysis of core-beam proton non-thermal features and their associated plasma instabilities. The evolution of temperature anisotropies and drift velocities are investigated in details. Properties of alpha particles, that have been investigated in previous Ulysses analysis [*Neugebauer et al.*, 1996; *Gary et al.*, 2002], and their associated instabilities will be the subject of a future work.

The paper is organized as it follows: in section 2 we describe the Ulysses data used in this analysis and the model adopted; in section 2.1 we report the observed radial trends of proton moments, discussing their main implications in terms of kinetic instabilities; section 3.1 reports the observed properties of the total proton distribution description, while 3.2 contains the analysis in the case of a two-population core-beam model; in section 4 we consider the role of the relative core-beam velocity in the stability of the plasma; we summarize the results in session 5 and, finally, in the conclusion (session 6) we discuss their outcome in the framework of solar wind models, as well as their implications for future observations and space missions.

2. Data analysis

Figure 1 shows the Ulysses trajectory in the plane of radial distance and latitude (left top), the radial distance as a function of time (right top), the observations as points in the plane of the radial distance and the solar wind velocity (left bottom), and the observations as points in the plane of $\nu_{pp}t_e$ - the product of the proton-proton collision frequency $\nu_{pp} \propto nT^{-3/2}$ and the transit time $t_e = R/v_{sw}$ - and the solar wind velocity (right bottom), for the dataset analyzed in this work, ∼150.000 data points. In the selected period, corresponding to the first Ulysses north pole passing during 1995-96, in a phase of solar minimum, the orbit of the spacecraft covered a radial distance from 1.3 to almost 5 AU, globally ranging from -30 to 80 degrees of heliographic latitude. During this scan Ulysses encountered mainly fast solar

wind, especially at high latitudes, while some slow wind was measured closer to the ecliptic, below 1.5 AU and beyond 4 AU. As shown in the bottom right panel, the Ulysses data display an anti-correlation between the bulk velocity and the estimated collisional rate $\nu_{pp}t_e$; Previous studies have shown that collisions can play a role in regulating the inter-species drifts up to $\nu_{pp}t_e \sim 0.1$ [*Neugebauer*, 1976; *Kasper et al.*, 2008]. The figure confirms that, while the observed slow wind has a variable and more relevant collisionality, the fast wind analyzed in this work (selected according to $v_{sw} > 630$ km/s, as shown in the lower panels of the figure by the dotted line) is essentially collisionless, so that we can reasonably associate the evolution of the observed non-thermal structures in proton distribution to interactions with waves/fluctuations of the plasma.

Proton data are obtained from the SWOOPS instrument on Ulysses [*Bame et al.*, 1992]; the integration time is of the order of some tens of seconds. Under typical conditions 2-4 spins are needed to obtain a full distribution function, each spin being 12s durations. Data points are taken every 4 or 8 minutes, depending on the spacecraft operation mode. Protons and alpha particles are separated by finding the energy channel between the proton and alpha particle peaks with the minimum total counts. This works most of the time as the proton and alpha particle peaks in energy/charge are separated by about a factor of two, but can fail in rare circumstances when the proton temperature is very high. A numerical deconvolution procedure is used to remove the instrument response from the proton and alpha particle distributions see Appendix A in *Neugebauer et al.* [2001] for a detailed description of the method. Following previous works [*Neugebauer et al.*, 2001; *Goldstein et al.*, 2010] we adopt two different models to describe the proton distribution functions: one model for the total distribution and a second model to represent the core-beam structure. For the first model, the properties of the proton distribution are obtained through summation in velocity space; this results in the velocity, the total density n_p and temperatures $T_{\parallel p}, T_{\perp p}$. The second model assumes a core-beam distribution based on two drifting bi-Maxwellian proton distributions; this is parametrized by: $n_c, T_{\parallel c}, T_{\perp c}$ for the core, $n_b, T_{\parallel b}, T_{\perp b}$ for the beam, by the differential velocity v_D between the two populations, and by the bulk velocity of the whole proton distribution. The parameter values are obtained by a least squares fit of the deconvolved phase space density estimates to the core-beam model. Subscripts p refers to the total distribution, while c and b refer to core and beam populations,

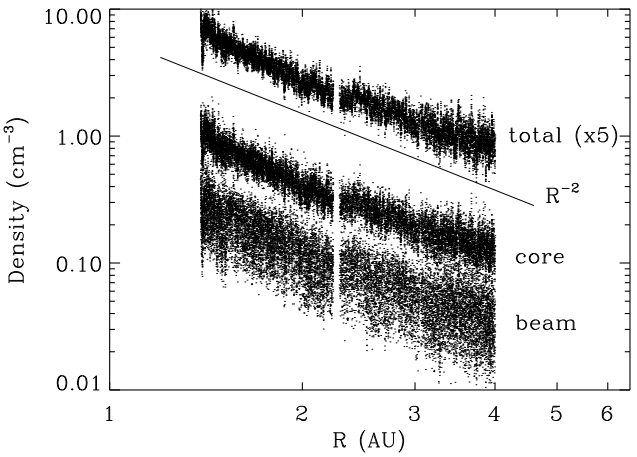

Figure 2. Density of total, core, and beam populations as a function of the radial distance in the fast wind.

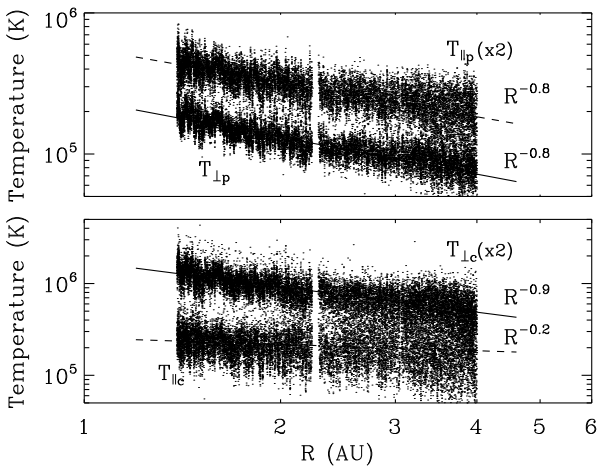

Figure 3. Parallel and perpendicular temperature profiles for total (top) and core (bottom) protons. Solid and dashed lines show the linear best fits for perpendicular and parallel temperatures, respectively.

respectively, and e to electrons. We define the plasma beta of each component i : $\beta_{\parallel,\perp i} = 8\pi n_i k_B T_{\parallel,\perp i}/B_0^2$. Moreover, since the two-populations model does not always fit successfully the proton distribution (i.e., when a slower dominant core and a faster more tenuous beam are not identified), we have restricted our analysis to the cases where $0.1n_e < n_b < 0.4n_e$. Note, however, that cases of "reversed" distributions with a more dense faster beam and a less dense slower one are typical for particular solar wind conditions (switchbacks), when a reversal in the magnetic field with respect to the dominant polarity is observed [*Neugebauer and Goldstein*, 2012]. These events, possibly associated to velocity shears [*Landi et al.*, 2006], are thus not included in the present analysis, but future investigations on the proton properties during magnetic field switchbacks cases are planned.

2.1. Radial profiles

In Figure 2 is shown the density radial dependence of the total distribution, as well as of core and beam separated

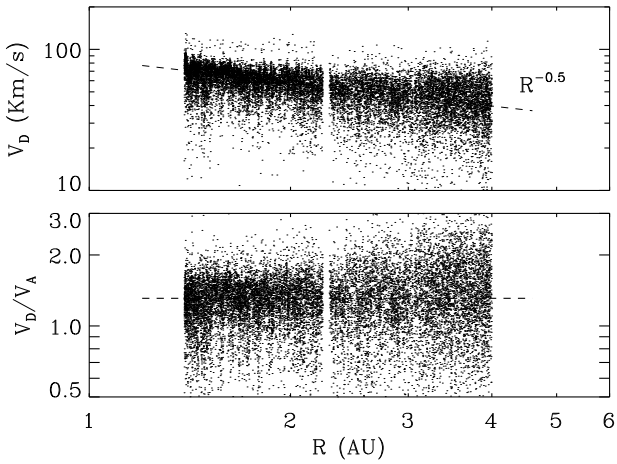

Figure 4. Core-beam drift velocity v_D as a function of distance, in km/s (top) and in units of v_A (bottom). Dashed lines displays the linear fit, $v_D \propto R^{-.5}$ and $v_D/v_A \sim$ const.

populations in the fast wind (note that the total density n_p is multiplied by a factor 5). All components approximatively fall off as R^{-2}, consistently with a spherical expansion at constant speed. However, it is worth noting that some departures in the slope can be observed when focusing on shorter intervals; in particular the total density profile shows a steeper slope between 1.5 and 2 AU than when considering data between 2 and 4 AU. A consistent evolution is observed also in the velocity profile (bottom left panel of Figure 1), showing a slight acceleration for R <2 AU and a deceleration at larger distances, so that density and velocity seem to radially vary preserving the total mass flux $F = R^2 n m_p v_{sw}$ [*Goldstein et al.*, 1996]. This behavior is likely due to some latitudinal dependence that is present in the dataset, as already discussed in the past [*McComas et al.*, 1995, 2003]

In a collisionless magnetized plasma, in the absence of interactions and heat fluxes, we expect two adiabatic invariants to be conserved [*Chew et al.*, 1956]:

$$\frac{T_\perp}{B} = \text{const.} \qquad \text{and} \qquad \frac{T_\parallel B^2}{n^2} = \text{const.} \tag{1}$$

This is so called double-adiabatic or CGL prediction. For a constant speed expansion in a radial magnetic field, as the observed polar wind in first approximation, the CGL predicts:

$$T_\perp \propto R^{-2} \qquad \text{and} \qquad T_\parallel = \text{const.} \tag{2}$$

Such a theoretical evolution for the proton temperatures in the absence of external interactions suggest two main comments. First, for a radial field, any $T_\perp$ slope observed weaker than R^{-2} indicates that some perpendicular heating is at work to contrast the rapid double-adiabatic perpendicular cooling, while any decrease of $T_\parallel$ reveals the presence of parallel cooling. Second, if relations (2) are satisfied all along the expansion, an increasing temperature anisotropy $T_\parallel > T_\perp$ is expected to develop with heliocentric distance in the plasma, becoming eventually unstable; this issue is addressed in the next section.

The first point can be investigated directly considering Figure 3, that shows the radial profiles of parallel and perpendicular temperatures for total (top) and core (bottom) population respectively (note that in the figure a factor is used to prevent the overlap of data points in the plots); solid and dashed lines correspond to the perpendicular and parallel, respectively, linear best fits: $T_{\parallel p}, T_{\perp p} \propto R^{-0.8}$ for the total population, and $T_{\parallel c} \propto R^{-0.2}$, $T_{\perp c} \propto R^{-0.9}$ for core protons. According to the evolution of total temperatures, based on the global distribution and so including the contribution of the kinetic energy of the drift velocity into the computation of the parallel temperature, both $T_{\parallel p}$ and $T_{\perp p}$ are observed to decrease with distance with a similar slope. In the approximation of a radial magnetic field, suitable for high latitudes and smaller distances in the Ulysses dataset, the slower than R^{-2} decrease of $T_{\perp p}$ indicates the presence of a perpendicular heating, and, at the same time, some additional parallel cooling is also needed to account for the decrease of $T_{\parallel p}$. The deductions based on the temperature profiles at large distances are in qualitative agreement with detailed Helios observations closer to the sun, where the same trends are observed in the fast wind between 0.3 and 1 AU [*Hellinger et al.*, 2011]. A more qualitative derivation of the external heating/cooling rates needed in the polar wind based on the present proton dataset is in preparation. Also, note that the protons exhibit typically $T_{\parallel p} > T_{\perp p}$ and that due to the similar scalings for both the temperatures, the total temperature anisotropy does not vary significantly with distance.

When considering the evolution of the proton core (Figure 3, bottom panel), we observe a majority of the opposite anisotropy, with $T_{\perp c} > T_{\parallel c}$. Moreover, while the perpendicular core temperature again decreases $\propto R^{-0.9}$ more slowly than the prediction R^{-2}, the parallel temperature of the core stays much closer to the double-adiabatic prediction, i.e., about constant with distance. This suggests that the proton heating observed in the total temperature profiles, and which is preferentially perpendicular, significantly affects the main core population. On the contrary there is also evidence that the complementary parallel cooling that is observed when taking into account the total distribution, is mainly connected to the dynamics of the secondary beam population, since such a cooling appears strongly reduced when restricting the analysis only to the core population. This is consistent with previous studies based on Helios data [e.g. *Marsch et al.*, 1982b; *Schwartz and Marsch*, 1983], where the decreasing of the total parallel temperature is observed to be related to the evolution of the relative drift velocity between core and beam with radial distance. Concerning Ulysses data, Figure 4 shows the drift velocity v_D as a function of radial distance (top panel) and the drift velocity v_D normalized to the local Alfvén velocity v_A as a function of radial distance (bottom panel); dashed lines show the fitted results $v_D \propto R^{-.5}$ and $v_D/v_A \sim$ const. Figure 4 clearly shows that the amplitude of v_D decreases with distance; note that in the CGL approximation, for a radial magnetic field, the relative drift is predicted to remain constant. When taking the relative drift normalized to the local Alfvén speed v_A, this ratio is not to be strongly dependent on the heliocentric distance and is mostly constrained between v_A and $2v_A$. This might be a signature of some kinetic processes, likely beam-type instabilities as these instabilities are typically destabilized when v_D is comparable to v_A. Also, it is interesting to note that in Helios data [*Hellinger et al.*, 2011, 2013] the cooling of the total parallel temperature driven by the beam deceleration can be responsible for a significant fraction of the perpendicular heating, via some mechanism that converts the kinetic energy of the core-beam drift into perpendicular thermal energy of particles. Again, this can be efficiently obtained by a pitch angle scattering due to ion-beam instabilities [*Matteini et al.*, 2012].

On the other hand, it is worth noting that the approximation of a radial field is limited to high latitudes and if considering a magnetic field described by a Parker spiral, the predictions by (1) lead to some different expectations at lower latitudes and larger distances. For a field decreasing more slowly than $1/R^2$, some parallel cooling is expected, so that at large distances one might derive a scaling of the total parallel temperature and of the drift velocity approximatively consistent with the observations, while in the perpendicular direction proton still need to be substantially heated also for a non radial field. Note that, on the other hand, in this case the nearly flat profile of the parallel temperature of the core population ($R^{-0.2}$) can not be explained. Consequently, some heating in both parallel and perpendicular directions is needed for core protons at larger heliocentric distances where the field becomes non radial. Such qualitative picture is consistent with the quantitative estimation of the proton heating and cooling rates obtained in Helios data [*Hellinger et al.*, 2011, 2013], showing that on the ecliptic, approaching 1 AU, the necessary parallel cooling rate observed closer to the Sun turns into a heating rate, as the angle of the Parker spiral becomes more significant.

A more qualitative analysis of the solar wind energetics with the Ulysses data is however complicated, since the radial profiles also contain a latitudinal dependence which is not well understood yet. For this reason in this paper we study the properties of protons and the related microphysics focusing on some particular parameter spaces where, comparing observations and theoretical thresholds, signatures of the activity of kinetic processes can be identified going beyond the radial evolution of the plasma.

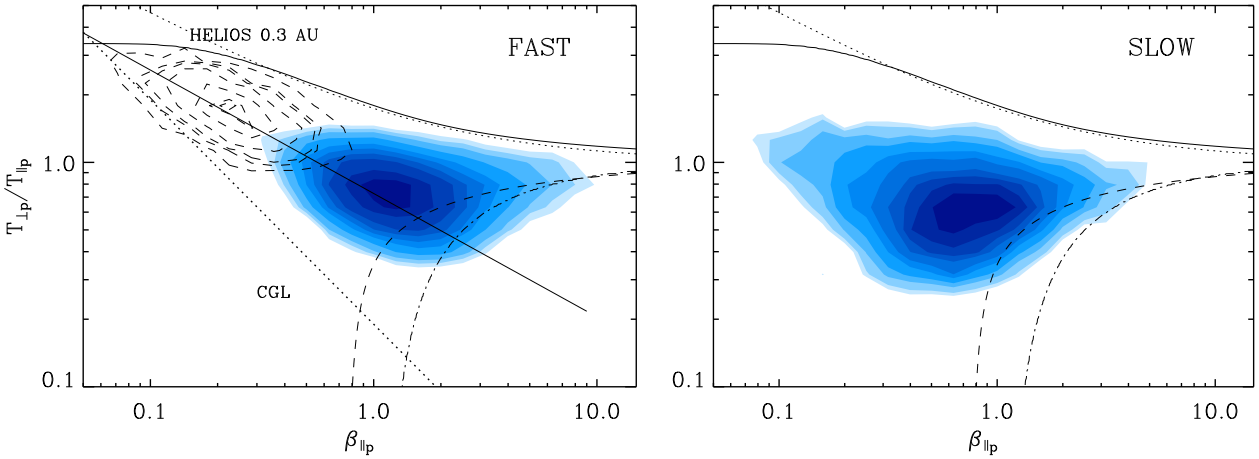

Figure 5. Single proton population analysis: observational counts of the total temperature anisotropy in the parameter space $(\beta_{\parallel p}, T_{\perp p}/T_{\parallel p})$, for fast (left) and slow (right) wind. The lowest contour level corresponds to 0.5% and 5% of the peak for fast and slow wind respectively. In both panels the thresholds of ion-cyclotron (solid), mirror (dotted), parallel fire hose (dashed), and oblique fire hose (dot-dashed) instabilities are shown. Dashed contours in left panel represents the distribution of Helios observations at 0.3 AU adapted from *Matteini et al.* [2007]. Solid line refers to the anti-correlation (3) and dotted line to the CGL prediction (2).

3. Temperature anisotropy

3.1. Total proton population

We start our analysis considering the case of the total population. Figure 5 shows the histograms of the observational counts in the parameter space $(\beta_{\parallel p}, T_{\perp p}/T_{\parallel p})$, for fast (left) and slow (right) wind. The lowest contour level corresponds to 5% and 0.5% of the peak for slow and fast wind respectively. In the same figure we show the linear theory predictions of the thresholds (or rather marginal stability relations with the maximum growth rate, γ_m, equal to 10^{-3} of the proton cyclotron frequency Ω_{cp}) for four kinetic instabilities driven by the proton temperature anisotropy: ion-cyclotron (solid), mirror (dotted), oblique (dash-dotted) and parallel (dashed) fire hoses. Here the linear predictions are computed for a plasma with isotropic electrons, bi-Maxwellian protons including a 5% of isotropic alpha particles, as in *Matteini et al.* [2007].

Slow wind observations are less frequent in the data set ($\sim$ 15.000 points, see Figure 1), and are plotted here only as a reference; the slow wind histogram however qualitatively reproduces the main features observed in more representative samples of WIND data discussed for example by *Hellinger et al.* [2006] and *Bale et al.* [2009]. Globally, the slow wind data are distributed around $\beta_{\parallel p} \sim 1$ and $T_{\perp p}/T_{\parallel p} \lesssim 1$, with a large spread; as discussed in *Matteini et al.* [2007], they show more localized clustering when shorter temporal analysis windows are selected (in order to select plasma with more uniform properties), so that the wide dispersion of distributions in the parameter space seems to be due to a combination of the very variable slow wind conditions (density, temperature, collisionality). Boundaries of the histogram show limits that are in reasonable agreement with the constraints predicted by the linear theory [see for example *Hellinger et al.*, 2006, for a discussion], especially at large betas; on the other hand, collisions are thought to be responsible for proton isotropization at low betas in the slow wind [*Bale et al.*, 2009]. Most of data show $T_{\parallel p} > T_{\perp p}$, which is the anisotropy expected at large distances, according to a spherical expansion in an nearly radial magnetic field. On the contrary, large $T_{\perp p} > T_{\parallel p}$ anisotropies are quite uncommon in the slow wind, being mainly correlated with the most collisionless plasma at 1 AU (cf. Figure 1 of *Bale et al.* [2009]); consistently with that, we do not find a significant fraction of $T_{\perp p} > T_{\parallel p}$ in the Ulysses observations for large distances, where is also likely that such anisotropy has been relaxed, through (at least partial) double-adiabatic cooling, as predicted by Eq. (2).

Fast wind data ($\sim$ 100.000 points, selected for the high latitudes > 30 deg) are shown in the color histogram of left panel of Figure 5. These data display a distribution which is consistent with the previous analysis based on data from a period of solar maximum (compare with Figure 1 of *Matteini et al.* [2007]). In the same panel, Helios data from fast solar wind protons observed at 0.3 (dashed contour) are also shown, as well as the anti-correlation between temperature anisotropy and parallel beta:

$$T_\perp/T_\parallel \propto \beta_\parallel^{-0.55} \tag{3}$$

found by *Marsch et al.* [2004] between 0.3 and 1 AU (solid line), and the CGL prediction for a radial field (dotted line).

As known from previous studies [e.g., *Marsch et al.*, 1982b], the solar wind plasma cools down more slowly than adiabatically, since the observed trajectory, mostly following the anti-correlation (3) in solid line, departs from equations (2), which assuming a spherical expansion for a radial magnetic field predict: $T_{\perp p}/T_{\parallel p} \propto 1/\beta_{\parallel p}$ (dotted line). Note that invoking a non radial magnetic field does not solve the inconsistency between theory and observations; assuming $B \propto R^{-1.6}$, a scaling consistent with the Ulysses magnetic data al large distance, leads to a predicted anisotropy $T_{\perp p}/T_{\parallel p} \propto 1/\beta_{\parallel p}^2$ so producing an even larger departure of the predicted trajectory from the observations [see *Matteini et al.*, 2012, for a more detailed discussion of the effects of a non radial field on the proton anisotropy evolution].

Moreover, the comparison between Helios and Ulysses data, reveals the progressive approach with distance of fast wind proton distribution to the fire hose unstable region, driven by the expansion. As already discussed in *Matteini et al.* [2007] the trajectory of protons in this parameter space after 1 AU departs from that observed at smaller distances (solid line) and indicates an evolution characterized by more isotropic temperatures. The trajectory traced in the $(\beta_{\parallel p}, T_{\perp p}/T_{\parallel p})$ plane is then in qualitative agreement with the marginal stability path constrained by a fire hose

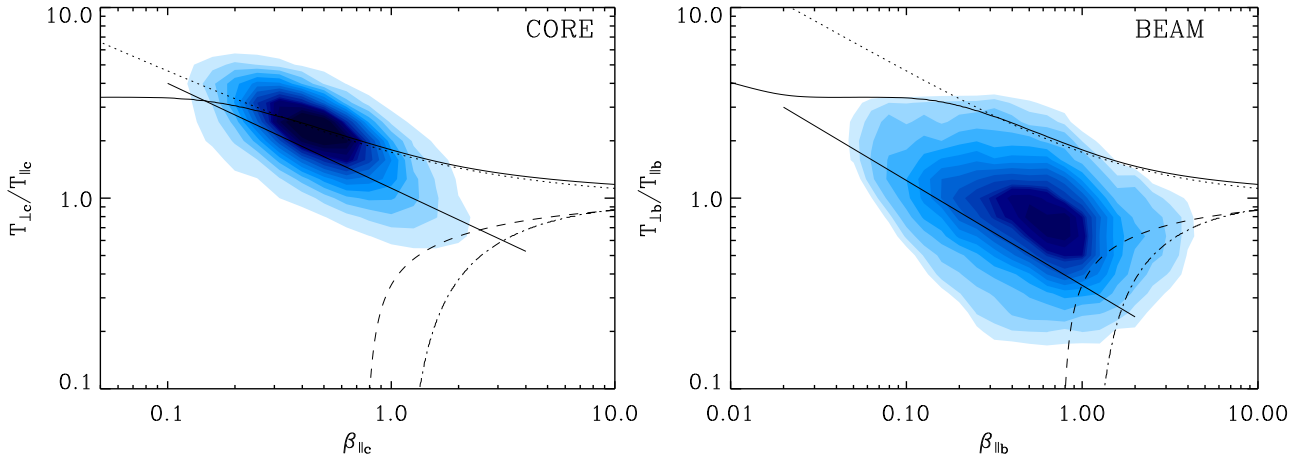

Figure 6. Observational counts of the temperature anisotropy in the parameter space $(\beta_\parallel, T_\perp/T_\parallel)$ for core (left) and beam (right) proton populations; lowest contour level corresponds to 5% of the peak. Instability thresholds are shown as in Figure 5. The solid line in both panels correspond to the anti-correlation found in Helios core protons (3).

instability, as suggested by numerical simulations that include the effects of the expansion on the ion thermal energetics [*Matteini et al.*, 2006; *Hellinger and Trávníček*, 2008]. This result is confirmed here using a larger data set and for a different solar wind condition (solar minimum).

Further indications of the activity of some kinetic instabilities is suggested by analyses of the local properties of Ulysses magnetic field spectra [*Wicks et al.*, 2010, 2013]. These show an enhancement of wave power when protons are closer to the instability threshold. Moreover, theoretical expectations for fire hose instabilities [*Hellinger and Trávníček*, 2008; *Matteini et al.*, 2012] predict such a power to be associated to k-vectors that are more aligned with the local magnetic field, in contrast with the dominant fluctuations associated to the perpendicular solar wind turbulent cascade. A confirmation of this prediction through a more detailed comparison between Ulysses particle and magnetic field data to infer the role of kinetic instabilities is in preparation (*Wicks et al., in prep*).

Despite the reasonable good agreement between data and theoretical predictions at this stage, the comparison still shows some discrepancies. This can be due to the limited assumption of a single anisotropic population, thus using total temperatures in the analysis, while the real distribution functions are more complicated and display at least two distinct ion populations. Consequently, we have extended our analysis of the linear stability of the proton velocity distribution functions to a more detailed core-beam distribution model.

3.2. Core-beam distribution

We consider now a different description for the proton distribution consisting of two distinct populations, a main core and a drifting beam, both modeled by a bi-Maxwellian distribution [*Goldstein et al.*, 2010]. As described in Section 2, we consider here only those cases where the fitting was successful in identifying core and beam populations with required properties. This leads to a subset of ~ 45.000 distributions. Note however that this does not mean that a secondary drifting population is not present in the excluded distributions; a structure aligned with the magnetic field is constantly observed in the data, but this is not always sufficiently resolved to make the adopted model converging.

In Figure 6, observations of the core and beam temperature anisotropy are shown. In the histograms the lowest contour level corresponds to 5% of the peak. Protons of the core distribution are characterized by $T_{\perp c} > T_{\parallel c}$, while beam protons show mainly $T_{\perp b} < T_{\parallel b}$. As a consequence, when plotted in the parameter space, the histograms of the observational counts display some differences with respect to the case of total temperatures.

We show in Figure 6 as reference the linear thresholds of the temperature-anisotropy driven instabilities as in Figure 5. Note, however, that these are computed for a single bi-Maxwellian proton velocity distribution function corresponding to the total proton population, so that some care must be used when comparing those thresholds to the observations of the core and beam populations, which are described as separated proton components. A more correct approach would imply computing the stability of one population against its anisotropy and beta, considering a multi-ion plasma (core, beam and alphas) and taking as external parameters the properties of the other populations. In practice this approach becomes very difficult to handle, due to the large numbers of parameters $(n_b/n_c, T_{\perp c}/T_{\parallel c}, T_{\perp b}/T_{\parallel b}, \beta_{\parallel c}, \beta_{\parallel b}, v_D$ and all the alpha properties) that can not be easily reduced in a two-dimensional space, so that we prefer to simply plot data with the usual thresholds, but making the reader aware of the approximation made.

Considering first the left panel of Figure 6, we note that the anisotropy of the core population is close to the ion-cyclotron and mirror thresholds and that some of the data points appear to be unstable when compared to the linear prediction for a single population bi-Maxwellian distribution (solid and dotted lines). As also inferred from Figure 3, large $T_{\perp c} > T_{\parallel c}$ anisotropies are observed mostly at closer distances to the Sun, while the value of the anisotropy relaxes with radial distance, in agreement with the expectation that the core is cooled down by the expansion. However, the observed variation of the core anisotropy is compatible with the slope inferred from Helios observations [*Marsch et al.*, 2004] (solid line) and is weaker than the double-adiabatic prediction. This supports further the idea that some processes must be at work in the plasma to perpendicular heat the plasma and counteract the adiabatic cooling driven by the expansion.

The temperature anisotropy of beam protons displays a larger dispersion in the parameter space, but mostly in the stable part. Also in this case, the anti-correlation between anisotropy and parallel beta (Eq. (3), solid line) is able to describe the trend of the observations, but not as well as in the core case. A closer inspection of the beam population

shows that the beam perpendicular temperature decreases more slowly ($\sim R^{-0.7}$) than the parallel ($\sim R^{-1}$), in contrast with the core temperatures. Those scalings are consistent with the analysis of *Goldstein et al.* [2010] on a smaller sample of Ulysses data, showing that the cooling with distance of the perpendicular temperature is faster for the core than for the beam, whereas the latter population has a stronger parallel cooling. Such an evolution, which is contrast with the double-adiabatic expectation $T_{\perp b}/T_{\parallel b} \propto R^{-2}$ for a radial field, may be explained by the presence of a mechanism able to regulate the properties of the beam population along the solar wind expansion, as for example, ion-beam instabilities [*Hellinger and Trávníček*, 2011]. We know from numerical simulations [*Daughton et al.*, 1999] that these processes lead to the perpendicular heating of the beam population as one of their main effects.

Moreover, the anisotropy of the beam population $T_{\perp b}/T_{\parallel b}$ appears well correlated with the core-beam drift velocity when normalized to the local Alfvén speed. This correlation, outlined for the first time by *Goldstein et al.* [2010], is here recovered and confirmed in Figure 8, where we show the observational count of observations in the plane $(T_{\perp b}/T_{\parallel b}, v_D/v_A)$. This validates the idea that the core-beam drift also plays a important role in regulating the level of anisotropy of the protons, and thus controlling the stability of the plasma; we focus on the evolution of the relative velocity between core and beam, and the associated instabilities in the next section.

4. Core-beam relative drift

Using a model based on two proton populations enables the analysis of the radial evolution of the velocity drift between the core and the beam. As discussed in section 2.1, v_D is observed to decrease with radial distance (Figure 4), however the drift velocity is also a function of the plasma properties and composition. In analogy to the temperature anisotropy, the stability of the core-beam structure can be effectively studied as a function of the plasma beta; both panels of Figure 7 show the observational count histogram of the core-beam drift normalized to the local Alfvén speed and $\beta_{\parallel c}$; as in the previous figure, the lowest contour level corresponds to 5% of the peak. According to a CGL evolution, we expect a direct correlation between $\beta_{\parallel c}$ and v_D/v_A. Since for a double-adiabatic system the parallel velocities are expected to follow the relation $v_D \propto n/B$ [e.g. *Matteini et al.*, 2012], and the Alfvén velocity $v_A \propto B/\sqrt{n}$, we then expect:

$$\frac{v_D}{v_A} \propto \frac{n^{3/2}}{B^2} \qquad \text{and} \qquad \beta_{\parallel c} \propto \frac{n^3}{B^4}\,, \tag{4}$$

so that one can simply predict:

$$\frac{v_D}{v_A} \propto \beta_{\parallel c}^{0.5}\,. \tag{5}$$

Note that, remarkably, this relation is independent from the profile of the magnetic field, so that it is expected to be valid for a generic interplanetary magnetic field.

The plot confirms the presence of a well defined correlation between the parameters; this is however not well described by the CGL prediction, Eq. (5), shown as the dotted line on Figure 7. On the contrary data appear to be bounded by an observational threshold, having a slope compatible with the relation: $v_D/v_A = 2.16{\beta_{\parallel c}}^{0.28}$, found between 0.3 and 1 AU in Helios data by *Tu et al.* [2004] and shown as a solid line (Figure 7, left panel). There is a slight shift between the *Tu et al.* [2004] analysis and our case, probably due to some systematic difference in computing the value of the temperatures, which contribute to the calculation of beta, but the slope of the correlation is very well reproduced, revealing a good agreement between Helios and Ulysses observations. Moreover, thanks to the large Ulysses statistical sample analyzed in this work, the shape of the data strongly suggests that the relation of *Tu et al.* [2004] can be interpreted as an observational constraint for protons in the $(\beta_{\parallel c}, v_D/v_A)$ plane rather than a simple correlation. The existence of such a direct correlation/boundary, extended over a large range of distances from the Sun, strongly suggests the presence of a mechanism able to regulate the value of the drift velocity during the solar wind plasma expansion. As pointed out by previous studies [e.g. *Marsch and Livi*, 1987; *Goldstein et al.*, 2000] this mechanism can be due to an ion-beam instability. While these instabilities are importantly controlled by the core beta and the drift velocity, these are not the only relevant parameters governing the beam instabilities, and as remarked in previous works, it is not trivial to find a combination of the plasma parameters which are able to explain the shape of observations (see for example Figure 2 of *Tu et al.* [2004]).

To outline this aspect, we have shown in the two panels of Figure 7 the linear predictions for the magnetosonic ion-beam instability [*Montgomery et al.*, 1975; *Daughton and Gary*, 1998] at parallel propagation, computed for two different combinations of plasma parameters. We have computed the linear dispersion for a plasma with two proton drifting populations, with densities $n_b = 0.2n_e$ and $n_c = 0.7n_e$ and alpha particles ($n_\alpha = 0.05n_e$). Electrons and alpha particles are considered isotropic, with $\beta_e = 1$ and $\beta_\alpha = 0.5$. In left panel, the dashed line corresponds to the isocontour of the maximum growth rate $\gamma_m = 10^{-2}\Omega_{cp}$ for a standard case, where isotropic proton populations are assumed and we have fixed the other plasma parameters; consistently with the results of *Tu et al.* [2004], this prediction does not provide a good agreement with the data. A significant shift of the threshold, improving the agreement with the observations can be obtained when considering anisotropic proton populations; in particular, it was shown by *Daughton and Gary* [1998] that a $T_{\perp b} < T_{\parallel b}$ temperature anisotropy in the beam distribution can enhance the instability growth rates at small drift velocities. Since the instability dependence on the beam anisotropy can be quite strong, keeping the latter fixed for the linear calculations is not completely suitable. As shown in Figure 8 these two parameters are correlated and when testing the linear stability for a given drift velocity, a related temperature anisotropy for the beam should be adopted. In order to better describe the solar wind conditions, we have considered in the linear theory realistic variations of the parameters reproducing the correlations observed and discussed in this study. Using equation (3), which reasonably describes correlations observed in Figure 6, we have expressed the proton parameters ($\beta_{\parallel b}$, $T_{\perp c}/T_{\parallel c}$, $T_{\perp b}/T_{\parallel b}$) as a function of $\beta_{\parallel c}$. These are: $T_{\perp c}/T_{\parallel c} = \beta_{\parallel c}^{-0.6}$, $T_{\perp b}/T_{\parallel b} = \beta_{\parallel c}^{0.3}$, and $\beta_{\parallel b} = \beta_{\parallel c}^{-0.3}/2.5$. Note that in the range of $\beta_{\parallel c}$ considered here, this leads to variations of these parameters within the most populated regions of the parameter space by the observations : $0.3 < \beta_{\parallel b} < 0.8$; $0.6 < T_{\perp c}/T_{\parallel c} < 4$; $0.5 < T_{\perp b}/T_{\parallel b} < 1.3$. We assumed a beam density of $n_b = 0.2n_e$. A relative drift of alphas with respect to protons is also included, with a velocity of $0.6v_A$ which is a quite representative value in the Ulysses dataset [*Goldstein et al.*, 2010]; however the results do not appear significantly sensitive to this parameter.

The resulting picture is shown in the right panel of the Figure 7, where the solid lines shows the isocontours of the maximum growth rate of the magnetosonic ion-beam instability for $\gamma_m = 10^{-3}, 10^{-2}, 10^{-1}\Omega_{cp}$. The agreement between data and theory is in this case reasonably good and seems to support the interpretation of the observed shape being constrained by the marginal stability of the magnetosonic ion-beam instability. However, some care must be

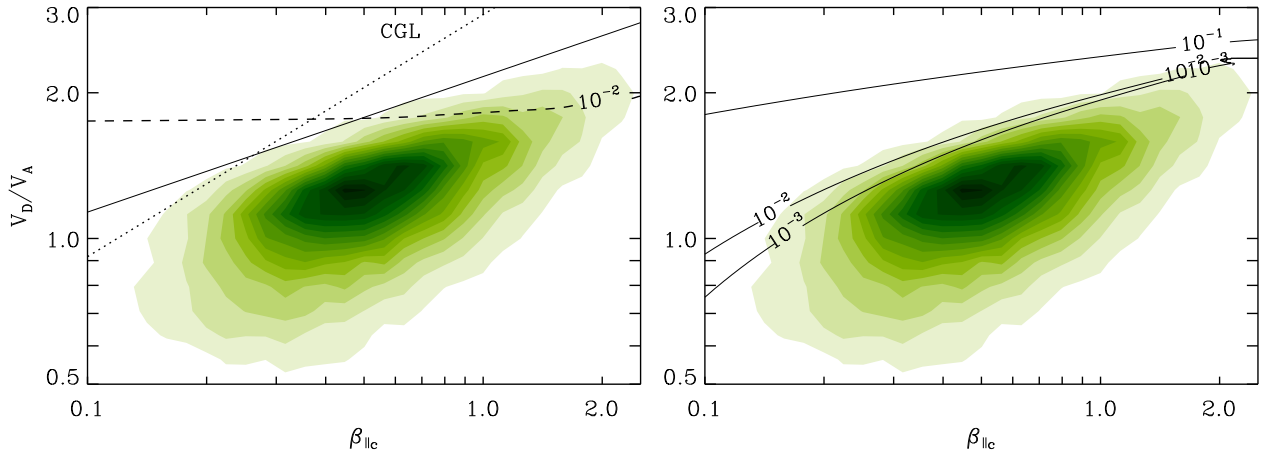

Figure 7. Histogram of the observational counts of the core-beam drift, normalized to the local Alfvén speed, as a function of the core parallel beta (both panels); lowest contour level corresponds to 5% of the peak. In left panel, the dotted line refers to the CGL prediction, relation (5), while the solid line represents the correlation observed in Helios data by *Tu et al.* [2004]; the linear theoretical $\gamma_m = 10^{-2}\Omega_{cp}$ level of the magnetosonic ion-beam instability with isotropic proton populations is shown in dashed line. In right panel the linear computation of the magnetosonic instability is obtained using a combination of parameters that empirically reproduces the trends observed in the Ulysses data: the solid lines show the $\gamma_m = 10^{-3}, 10^{-2}, 10^{-1}\Omega_{cp}$ levels of the instability.

used when interpreting this result; even if this is not an *ad hoc* choice of the parameters, since they are derived from the observed solar wind trends, different combinations of those may significantly affect the agreement. On other hand, the fact that adopting more realistic parameters and their trends pushes the linear threshold/marginal stability constraints in a direction which approaches the observed bounds is quite encouraging, and suggests that similar techniques might be useful for future studies.

5. Discussion

According to the observations presented in this work, the radial temperature profiles of both the total and the distinct core-beam proton populations suggest the presence of wave-particle interactions that influence the thermodynamics of ions during the expansion. Parallel and perpendicular temperatures of the total distribution are observed to decrease with a similar slope, with significant departure from the double-adiabatic/CGL expectation (2). For core protons the perpendicular temperature decreases faster than the parallel, which on the contrary displays a much flatter profile. This suggests that the parallel component of the core follows a more adiabatic-like evolution, while in the direction perpendicular to the magnetic field, protons need to be significantly heated. For the beam population, stronger departures are observed, since the parallel temperature is found to decrease slightly faster than the perpendicular.

Total temperature anisotropies observed at solar minimum (Fig. 5) reproduce well the evolution path in the parameter space ($\beta_{\parallel p}$,$T_{\perp p}/T_{\parallel p}$) found in Ulysses data at solar maximum [*Matteini et al.*, 2007], confirming that a fire hose instability is likely at work in constraining the proton anisotropy after 1 AU. This is consistent with the observation of enhanced magnetic field fluctuations in the same dataset during periods when the plasma is closer to the unstable regions in the parameter space ($\beta_{\parallel p}, T_{\perp p}/T_{\parallel p}$) [*Wicks et al.*, 2013]. At the same time, the core of the distributions, which exhibit a significant $T_{\perp c} > T_{\parallel c}$ anisotropy, is possibly unstable to ion-cyclotron instability (Fig. 6). Such an instability may constitute a constrain to the amount of $T_{\perp c} > T_{\parallel c}$ anisotropy that can be generated though the perpendicular heating needed in the solar wind to explain the proton temperature profiles [e.g., *Hellinger et al.*, 2011], and which is likely provided by the interaction of protons with plasma waves and/or turbulence [e.g. *Chandran et al.*, 2010].

The core-beam relative drift is observed to decrease with distance faster than adiabatic, providing an explanation for the rapid decrease observed in the parallel temperature of the total proton distribution. During the expansion the regulation of the relative velocity of the secondary population with respect to the main core is likely due to an ion-beam instability and this produces also some different scalings in the core and beam temperature with distance, as also preliminarily discussed by *Goldstein et al.* [2010]. In this kind of process part of the kinetic energy associated with the relative speed of core and beam is converted into thermal energy of each population, leading to a preferential perpendicular heating, at the cost of drift relaxation, and producing a change in the particle anisotropies, in particular for the more dilute population (proton beam or alpha particles) [*Matteini et al.*, 2012]. The observational need for a kinetic mechanism

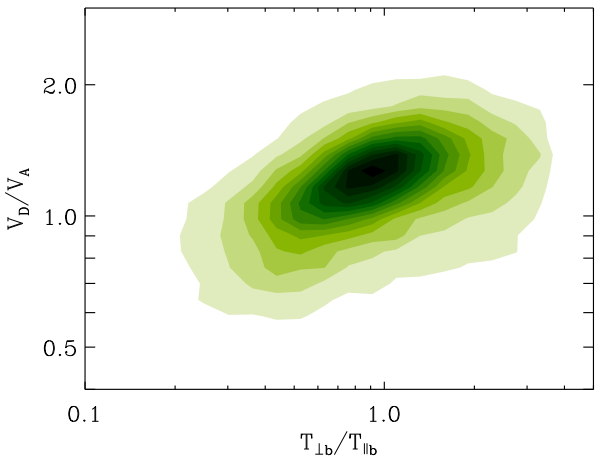

Figure 8. Correlation between the proton core-beam drift, in units of v_A, and the temperature anisotropy of the beam population, after *Goldstein et al.* [2010]. Lowest contour level corresponds to 5% of the histogram peak.

transferring energy from the parallel to the perpendicular direction along the expansion of the fast solar wind has been recently inferred by *Hellinger et al.* [2011] and an ion-beam type instability is a strong candidate for this role [*Schwartz et al.*, 1981; *Hellinger and Trávníček*, 2011].

A possible direct signature for such a dynamics is the presence of a well defined observational limit in the left panel of Figure 7. In the ($\beta_{\|c}$,v_D/v_A) parameter space, protons appear to be bounded by a threshold (solid line) that departs from the CGL prediction of relation (5, dotted line). The same correlation was observed also in Helios data closer to the Sun. We have shown, for the first time, that such an evolution of protons is compatible with the constraints of linear Vlasov theory of the magnetosonic ion-beam instability when parameter correlations consistent with those observed in the solar wind are used. This result suggests that this instability is at work in the solar wind, and that the observed core-beam relative drift evolution is regulated by its activity.

It is important to note that the magnetosonic instability, unlike fire hose, does not need large betas to be excited; our calculation in Fig. 7 is shown for $\beta_{\|c} > 0.1$, but the unstable region extends also to lower betas. Moreover, other ion-beam instabilities at oblique propagation are predicted to be play a role at small beta [*Daughton and Gary*, 1998]. Consequently, these processes can also be at work closer to the Sun. This seems to be confirmed by the Helios observations of *Tu et al.* [2004] that reveal the presence of a correlation between $\beta_{\|p}$ and v_D/v_A already between 0.3 and 1 AU, and supported by the fact that proton drifts that are comparable to the local Alfvén speed are observed already at small heliocentric distances. Progressively, as the plasma expands and the proton temperatures evolve, proton distributions approach the fire hose unstable region at larger distances (typically for $\beta_{\|p} \sim 1$ at 1 AU), where observations suggest that the proton anisotropy starts to be further regulated by this instability. Note that a secondary effect of the fire hose activity can be also the destruction of the core-beam structure, due to the strong pitch angle scattering of protons by unstable fluctuations [*Hellinger and Trávníček*, 2011].

6. Conclusion

We have presented a large statistical study of non thermal ion properties in the solar wind, based on Ulysses observations between 1.3 and 5 AU during the solar minimum of activity. The analysis focused on the temperature anisotropy of core and beam proton populations, as well as their relative drift, as a function of distance and of plasma parameters. Kinetic instabilities associated with these non thermal features have been investigated in detail. Our results confirm that a fire hose instability plays a major role in constraining the proton anisotropy during the solar wind expansion, in agreement with theoretical predictions [*Matteini et al.*, 2006; *Hellinger and Trávníček*, 2008], and suggests that a magnetosonic ion-beam instability is also at work in the solar wind, shaping the core-beam proton structure as a function of the radial distance.

The combined analysis of the present results with previous Helios/Ulysses studies [*Gary et al.*, 2002; *Marsch et al.*, 2004; *Tu et al.*, 2004; *Matteini et al.*, 2007], makes it possible to derive some general properties of the evolution of proton distributions in the fast solar wind. According to these findings, a significant part of the observed protons are found close to an instability threshold (fire hose, ion-beam and possibly mirror or ion-cyclotron for proton cores); one could then argue that for a significant fraction of the time the fast solar wind plasma at large distances is influenced and constrained by wave-particle interactions. This makes the investigation of the role of such processes absolutely necessary in order to infer from observational trends (e.g., temperature profiles) informations about the proton energetics and the contribution by additional source of heating (i.e., turbulence), since all those quantities would be largely dependent on the wave-particle effects for most of the time and distances.

Such a global picture, outlining a non trivial evolution of ion distributions with distance, also strongly indicates that microphysics effects have to be retained in solar wind fluid models in order obtain a realistic description of the plasma. For example, in a model recently presented by *Chandran et al.* [2011], constraints imposed by temperature anisotropy driven instabilities are taken into account in the large scale wind evolution. In this framework, the parallel cooling provided by the regulation of the core-beam drift through ion-beam instability presented in this work, should be included as well in order to efficiently control the thermal energetics of ions along the magnetic field.

Moreover, kinetic instabilities may also contribute to the evolution of magnetic structures that are frequently observed in the solar wind plasma. It is known that temperature anisotropy is expected to modify the growth rate of the tearing instability [*Chen and Palmadesso*, 1984], thus influencing the stability of current sheets and the associated magnetic reconnection activity. Preliminary numerical simulations of the coupling between microscale processes driven by temperature anisotropy and the intermediate solar wind magnetic structures [*Matteini et al.*, 2013] suggest that fluctuations generated by kinetic instabilities (like those at work in the solar wind), play a role in regulating the stability and evolution of current sheets in anisotropic non homogenous plasmas. This aspect should also be addressed in more detail in the future.

We finally note that the agreement between data and linear theory presented in this work, particularly in the case of the core population in Fig. 6, is still not fully satisfactory; this is not surprising since the thresholds used as references are computed for a bi-Maxwellian population, while the real distributions are more complicated and this can introduce changes in the instability thresholds [e.g. *Isenberg*, 2012]. On the other hand, we have shown that considering a more realistic description of the plasma, with correlated velocity drifts and different core-beam temperature anisotropies in the Vlasov dispersion as we have done for the analysis of the drift properties in section 4, significantly improves the comparison between theory and observations. However, ideally, a detailed analysis of the stability of the plasma based on the local plasma dispersion as derived, for each measurement, from the moments of the observed distribution, would be then more suitable, even if more computationally costly. In this direction, preliminary tests of the stability of the plasma based on the local parameters, that we have performed on a smaller sample of the data indicate that this procedure does not completely solve the discrepancy between theoretical linear thresholds and observations in Fig. 6. This suggests that in some cases considering only moments of the distributions can be not accurate enough, and that the overall stability of the plasma may crucially depend on the details of the distribution function (e.g., presence of plateaux, secondary peaks, and holes) since kinetic instabilities have a resonant nature. Also, we have not taken into account in this work the possible influence of waves and turbulence on the distribution measurements, which might introduce some apparent temperature anisotropy [*Verscharen and Marsch*, 2011; *Nariyuki*, 2012]. The next generation of spacecraft characterized by shorter time window for plasma measurements will also contribute to clarify this aspect.

In conclusion, more theoretical work, including numerical simulations, has to be done to better constrain the role of kinetic instabilities in regulating the observed anisotropy, and more precise in situ particle observations are needed as well. Observations provided by the high resolution instruments of the forthcoming missions as Solar Orbiter and Solar Probe Plus will be helpful in this task.

Acknowledgments. The authors thank Roland Grappin, Tim Horbury and Robert Wicks for useful discussions. The research leading to these results has received funding from the European Commission's Seventh Framework Programme (FP7) under the grant agreement SHOCK (project number 284515), and from the Science and Technology Facilities Council (STFC). PH acknowledges the grant P209/12/2023 of the Grant Agency of the Czech Republic. The research described in this paper was also carried out in part at the Jet Propulsion Laboratory, California Institute of Technology, under a contract with the National Aeronautics and Space Administration".

References

Antonucci, E. (2006), Wind in the Solar Corona: Dynamics and Composition, *Space Sci. Rev.*, *124*, 35–50, doi:10.1007/s11214-006-9098-6.

Araneda, J. A., E. Marsch, and A. F.-Viñas (2008), Proton Core Heating and Beam Formation via Parametrically Unstable Alfvén-Cyclotron Waves, *Phys. Rev. Lett.*, *100*(12), 125003, doi:10.1103/PhysRevLett.100.125003.

Araneda, J. A., Y. Maneva, and E. Marsch (2009), Preferential Heating and Acceleration of α Particles by Alfvén-Cyclotron Waves, *Phys. Rev. Lett.*, *102*(17), 175001, doi:10.1103/PhysRevLett.102.175001.

Bale, S. D., J. C. Kasper, G. G. Howes, E. Quataert, C. Salem, and D. Sundkvist (2009), Magnetic Fluctuation Power Near Proton Temperature Anisotropy Instability Thresholds in the Solar Wind, *Phys. Rev. Lett.*, *103*(21), 211,101–+, doi:10.1103/PhysRevLett.103.211101.

Bame, S. J., D. J. McComas, B. L. Barraclough, J. L. Phillips, K. J. Sofaly, J. C. Chavez, B. E. Goldstein, and R. K. Sakurai (1992), The ulysses solar wind plasma experiment, *A&AS*, *92*, 237–265.

Chandran, B. D. G., B. Li, B. N. Rogers, E. Quataert, and K. Germaschewski (2010), Perpendicular Ion Heating by Low-frequency Alfvén-wave Turbulence in the Solar Wind, *ApJ*, *720*, 503–515, doi:10.1088/0004-637X/720/1/503.

Chandran, B. D. G., T. J. Dennis, E. Quataert, and S. D. Bale (2011), Incorporating Kinetic Physics into a Two-fluid Solar-wind Model with Temperature Anisotropy and Low-frequency Alfvén-wave Turbulence, *ApJ*, *743*, 197, doi:10.1088/0004-637X/743/2/197.

Chen, J., and P. Palmadesso (1984), Tearing instability in an anisotropic neutral sheet, *Phys. Fluids*, *27*, 1198–1206, doi:10.1063/1.864727.

Chew, G. F., M. L. Goldberger, and F. E. Low (1956), The boltzmann equation and the one-fluid fydromagnetic equations in the absence of particle collisions, *Proc.Roy.Soc. London*, *236*, 112.

Daughton, W., and S. P. Gary (1998), Electromagnetic proton/proton instabilities in the solar wind, *J. Geophys. Res.*, *103*, 20,613–20,620.

Daughton, W., S. P. Gary, and D. Winske (1999), Electromagnetic proton/proton instabilities in the solar wind: Simulations, *J. Geophys. Res.*, *104*, 4657–4668, doi:10.1029/1998JA900105.

Gary, S. P., B. E. Goldstein, and J. T. Steinberg (2001), Helium ion acceleration and heating by Alfvén/cyclotron fluctuations in the solar wind, *J. Geophys. Res.*, *106*, 24,955–24,964.

Gary, S. P., B. E. Goldstein, and M. Neugebauer (2002), Signatures of wave-ion interactions in the solar wind: Ulysses observations, *J. Geophys. Res.*, *107*, 4–1, doi:10.1029/2001JA000269.

Goldstein, B. E., M. Neugebauer, J. L. Phillips, S. Bame, J. T. Gosling, D. McComas, Y. . Wang, N. R. Sheeley, and S. T. Suess (1996), Ulysses plasma parameters: latitudinal, radial, and temporal variations., *A&A*, *316*, 296–303.

Goldstein, B. E., M. Neugebauer, L. D. Zhang, and S. P. Gary (2000), Observed constraint on proton-proton relative velocities in the solar wind, *Geophys. Res. Lett.*, *27*, 53–56.

Goldstein, B. E., M. Neugebauer, and X. Zhou (2010), Ulysses Observations of the Properties of Multiple Ion Beams in the Solar Wind, *Twelfth International Solar Wind Conference*, *1216*, 261–264, doi:10.1063/1.3395851.

Hellinger, P., and P. M. Trávníček (2008), Oblique proton fire hose instability in the expanding solar wind: Hybrid simulations, *J. Geophys. Res.*, *113*, A10109, doi:10.1029/2008JA013416.

Hellinger, P., and P. M. Trávníček (2011), Proton core-beam system in the expanding solar wind: Hybrid simulations, *J. Geophys. Res.*, *116*, A11101, doi:10.1029/2011JA016940.

Hellinger, P., M. Velli, P. Trávníček, S. P. Gary, B. E. Goldstein, and P. C. Liewer (2005), Alfvén wave heating of heavy ions in the expanding solar wind: Hybrid simulations, *J. Geophys. Res.*, *110*, A12109, doi:10.1029/2005JA011244.

Hellinger, P., P. Trávníček, J. C. Kasper, and A. J. Lazarus (2006), Solar wind proton temperature anisotropy: Linear theory and WIND/SWE observations, *Geophys. Res. Lett.*, *33*, L09101, doi:10.1029/2006GL025925.

Hellinger, P., L. Matteini, Š. Štverák, P. M. Trávníček, and E. Marsch (2011), Heating and cooling of protons in the fast solar wind between 0.3 and 1 AU: Helios revisited, *J. Geophys. Res.*, *116*, A09105, doi:10.1029/2011JA016674.

Hellinger, P., Š. Štverák, P. M. Trávníček, L. Matteini, and M. Velli (2013), Proton thermal energetics in the solar wind: Helios reloaded, *J. Geophys. Res.*, doi:10.1029/2012JA018205.

Isenberg, P. A. (2012), A self-consistent marginally stable state for parallel ion cyclotron waves, *Phys. Plasmas*, *19*(3), 032,116, doi:10.1063/1.3697721.

Kasper, J. C., A. J. Lazarus, and S. P. Gary (2002), Wind/swe observations of firehose constraint on solar wind proton temperature anisotropy, *Geophys. Res. Lett.*, *29*, 1839, doi:10.1029/2002GL015128.

Kasper, J. C., A. J. Lazarus, and S. P. Gary (2008), Hot solar-wind helium: Direct evidence for local heating by alfvén-cyclotron dissipation, *prl*, *101*(26), 261103, doi:10.1103/PhysRevLett.101.261103.

Landi, S., P. Hellinger, and M. Velli (2006), Heliospheric magnetic field polarity inversions driven by radial velocity field structures, *Geophys. Res. Lett.*, *33*, L14101, doi:10.1029/2006GL026308.

Landi, S., L. Matteini, and F. Pantellini (2012), On the Competition Between Radial Expansion and Coulomb Collisions in Shaping the Electron Velocity Distribution Function: Kinetic Simulations, *ApJ*, *760*, 143, doi:10.1088/0004-637X/760/2/143.

Marsch, E., and S. Livi (1987), Observational evidence for marginal stability of solar wind ion beams, *J. Geophys. Res.*, *92*, 7263–7268.

Marsch, E., H. Rosenbauer, R. Schwenn, K.-H. Muehlhaeuser, and F. M. Neubauer (1982a), Solar wind helium ions - Observations of the HELIOS solar probes between 0.3 and 1 AU, *J. Geophys. Res.*, *87*, 35–51.

Marsch, E., R. Schwenn, H. Rosenbauer, K.-H. Muehlhaeuser, W. Pilipp, and F. M. Neubauer (1982b), Solar wind protons - Three-dimensional velocity distributions and derived plasma parameters measured between 0.3 and 1 AU, *J. Geophys. Res.*, *87*, 52–72.

Marsch, E., X.-Z. Ao, and C.-Y. Tu (2004), On the temperature anisotropy of the core part of the proton velocity distribution function in the solar wind, *J. Geophys. Res.*, *109*, A04102, doi:10.1029/2003JA010330.

Marsch, E., L. E. Zhao, and C.-Y. Tu (2006), Limits on the core temperature anisotropy of solar wind protons, *Annales Geophysicae*, *24*, 2057–2063.

Maruca, B. A., J. C. Kasper, and S. P. Gary (2012), Instability-driven Limits on Helium Temperature Anisotropy in the Solar Wind: Observations and Linear Vlasov Analysis, *ApJ*, *748*, 137, doi:10.1088/0004-637X/748/2/137.

Matteini, L., S. Landi, P. Hellinger, and M. Velli (2006), Parallel proton fire hose instability in the expanding solar wind: Hybrid simulations, *J. Geophys. Res.*, *111*, A10101, doi:10.1029/2006JA011667.

Matteini, L., S. Landi, P. Hellinger, F. Pantellini, M. Maksimovic, M. Velli, B. E. Goldstein, and E. Marsch (2007), Evolution of the solar wind proton temperature anisotropy from 0.3 to 2.5 AU, *Geophys. Res. Lett.*, *34*, L20105, doi:10.1029/2007GL030920.

Matteini, L., S. Landi, L. Del Zanna, M. Velli, and P. Hellinger (2010a), Parametric decay of linearly polarized shear Alfvén waves in oblique propagation: one and two-dimensional hybrid simulations, *Geophys. Res. Lett.*, *37*, doi:10.1029/2010GL044806.

Matteini, L., S. Landi, M. Velli, and P. Hellinger (2010b), Kinetics of parametric instabilities of Alfvén waves: evolution of ion distribution functions, *J. Geophys. Res.*, *115*, doi: 10.1029/2009JA014987.

Matteini, L., P. Hellinger, S. Landi, P. Trávnícek, and M. Velli (2012), Ion kinetics in the solar wind: Coupling global expansion to local microphysics, *Space Sci. Rev.*, *172*, 373, doi: 10.1007/s11214-011-9774-z.

Matteini, L., S. Landi, M. Velli, and W. H. Matthaeus (2013), Proton Temperature Anisotropy and Magnetic Reconnection in the Solar Wind: Effects of Kinetic Instabilities on Current Sheet Stability, *ApJ*, *763*, 142, doi:10.1088/0004-637X/763/2/142.

McComas, D. J., B. L. Barraclough, J. T. Gosling, C. M. Hammond, J. L. Phillips, M. Neugebauer, A. Balogh, and R. J. Forsyth (1995), Structures in the polar solar wind: Plasma and field observations from ulysses, *J. Geophys. Res.*, *100*(9), 19,893–19,902.

McComas, D. J., H. A. Elliott, N. A. Schwadron, J. T. Gosling, R. M. Skoug, and B. E. Goldstein (2003), The three-dimensional solar wind around solar maximum, *Geophys. Res. Lett.*, *30*, 24–1, doi:10.1029/2003GL017136.

Montgomery, M. D., S. P. Gary, D. W. Forslund, and W. C. Feldman (1975), Electromagnetic ion-beam instabilities in the solar wind, *Phys. Rev. Lett.*, *35*, 667–670, doi: 10.1103/PhysRevLett.35.667.

Nariyuki, Y. (2012), On apparent temperature in low-frequency Alfvénic turbulence, *Phys. Plasmas*, *19*(8), 084,504, doi: 10.1063/1.4747499.

Neugebauer, M. (1976), The role of Coulomb collisions in limiting differential flow and temperature differences in the solar wind, *J. Geophys. Res.*, *81*, 78–82, doi:10.1029/JA081i001p00078.

Neugebauer, M., and B. E. Goldstein (2012), Double-Proton Beams and Magnetic Switchbacks in the Solar Wind, in *Proc. of the Thirteenth International Solar Wind Conference*, American Institute of Physics Conference Series.

Neugebauer, M., B. E. Goldstein, E. J. Smith, and W. C. Feldman (1996), Ulysses observations of differential alpha-proton streaming in the solar wind, *J. Geophys. Res.,* , *101*, 17,047–17,056, doi:10.1029/96JA01406.

Neugebauer, M., B. E. Goldstein, D. Winterhalter, E. J. Smith, R. J. MacDowall, and S. P. Gary (2001), Ion distributions in large magnetic holes in the fast solar wind, *J. Geophys. Res.*, *106*, 5635–5648, doi:10.1029/2000JA000331.

Schwartz, S. J., and E. Marsch (1983), The radial evolution of a single solar wind plasma parcel, *J. Geophys. Res.*, *88*, 9919–9932.

Schwartz, S. J., W. C. Feldman, and S. P. Gary (1981), The source of proton anisotropy in the high-speed solar wind, *J. Geophys. Res.*, *86*, 541–546, doi:10.1029/JA086iA02p00541.

Tu, C.-Y., E. Marsch, and Z.-R. Qin (2004), Dependence of the proton beam drift velocity on the proton core plasma beta in the solar wind, *J. Geophys. Res.*, *109*, A05101, doi: 10.1029/2004JA010391.

Štverák, Š., P. Trávníček, M. Maksimovic, E. Marsch, A. N. Fazakerley, and E. E. Scime (2008), Electron temperature anisotropy constraints in the solar wind, *J. Geophys. Res.*, *113*, A03103, doi:10.1029/2007JA012733.

Verscharen, D., and E. Marsch (2011), Apparent temperature anisotropies due to wave activity in the solar wind, *Ann. Geophys.*, *29*, 909–917, doi:10.5194/angeo-29-909-2011.

Wicks, R. T., T. S. Horbury, C. H. K. Chen, and A. A. Schekochihin (2010), Power and spectral index anisotropy of the entire inertial range of turbulence in the fast solar wind, *MNRAS*, *407*, L31–L35, doi:10.1111/j.1745-3933.2010.00898.x.

Wicks, R. T., L. Matteini, T. S. Horbury, P. Hellinger, and A. D. Roberts (2013), Temperature anisotropy instabilities; combining plasma and magnetic field data at different distances from the Sun, *Proc. of the Thirteenth International Solar Wind Conference*.

L. Matteini, Imperial College London, London, SW7 2AZ, UK

P. Hellinger, Astronomical Institute, AS CR, CZ-14131 Prague, Czech Republic.

B. Goldstein, Jet Propulsion Laboratory, California Institute of Technology, 4800 Oak Grove Drive, Pasadena, CA 91109, USA.

S. Landi, Dipartimento di Fisica e Astronomia, Università degli Studi di Firenze, Largo E. Fermi 2, 50125 Firenze, Italy.

M.Velli, Jet Propulsion Laboratory, California Institute of Technology, 4800 Oak Grove Drive, Pasadena, CA 91109, USA.

M. Neugebauer, Lunar and Planetary Laboratory, 1629 E. University Blvd., Tucson, AZ 85721-0092